Journal of Bio- and Tribo-Corrosion (2020) 6:5
https://doi.org/10.1007/s40735-019-0291-z

Synthesis, Characterization and Inhibition Performance of Schiff Bases for Aluminium Corrosion in 1 M H_2SO_4 Solution

R. S. Nathiya[1] · Suresh Perumal[2] · Malathy Moorthy[1] · Vajjiravel Murugesan[3] · Rajavel Rangappan[1] · V. Raj[1]

Received: 22 May 2019 / Revised: 30 August 2019 / Accepted: 26 September 2019 / Published online: 1 November 2019
© Springer Nature Switzerland AG 2019

Abstract

The corrosion inhibition efficiency of newly synthesized Schiff bases, SB-1 [(4E)-*N*-((Z)-2-((furan-2-yl)methylimino) indolin-3-ylidene)(furan-2-yl)methanamine] and SB-2 [(7Z,8Z)-6-chloro-N2,N4-bis(1-(pyridin-2-yl)ethylidene)pyrimidine-2,4-diamine], was investigated for aluminium corrosion in 1 M H_2SO_4 medium using mass loss and electrochemical techniques. Potentiodynamic polarization curves show that addition of Schiff bases in the acid solution shifts the corrosion potential (E_{corr}) towards positive direction, suggesting that chosen SBs are performed as mixed-type inhibitiors. The adsorption process of Schiff bases on aluminium surface obeys Langmuir isotherm. Further, electrochemical impedance studies (EIS) reveal that the inhibition efficiency remarkably rises with increasing SBs concentration and the maximum inhibition efficiencies of 97% and – 95% were obtained for SB-1 and SB-2, respectively, for the inhibitor concentration of 500 ppm. Additionally, the associated activation parameters and thermodynamic data of adsorption were evaluated. Scanning electron microscope (SEM) studies further confirm that ligands of SB-1 and SB-2 have a strong tendency to adhere on top of aluminium and protect its corrosion against acidic media.

Graphic Abstract

The SEM micrographs of corroded and inhibited aluminium surfaces and the maximum inhibition efficiency of aluminium corrosion are achieved to be 97% for Schiff bases (SB-1) in 1 M H_2SO_4 solution with the concentration of 500 ppm.

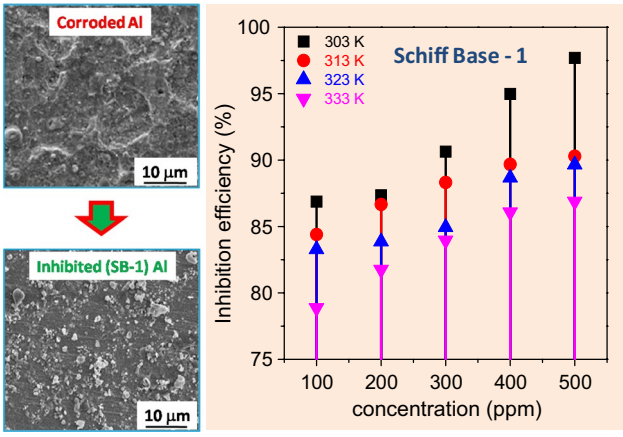

Keywords Aluminium · Schiff bases · Adsorption · EIS · Potentiodynamic polarization · SEM

1 Introduction

Aluminium corrosion is one of the major issues that often occur in many industries and can also lead to serious damages, causing the economic consequences which are related

✉ V. Raj
alaguraj2@rediffmail.com

Extended author information available on the last page of the article

to repair, replacement and product losses. Additionally, aluminium and its alloys are viewed to be a great interest due to their cost-effectiveness, high electrical/thermal conductivities and high energy density [1–4]. Generally, formation of a stable protective thin film layer of aluminium oxide on top of aluminium metal prevents aluminium corrosion for some extend and makes them as corrosive-resistant materials; however, these formed passive/protective layers are of amphoteric in nature and could easily get dissolved against strong acidic (HCl, HNO_3 and H_2SO_4) or alkaline (NaOH/NaCl) environment, wherein hydrogen evolution/product of aluminate ion arises by conjugate cathodic processes during corrosion [5–13]. Thus, many significant attempts were employed in a concern with protecting aluminium and its alloys against strongly acidic and alkaline environment, among which utilization of corrosion inhibitor is regarded as most commonly used corrosion protective process or corrosion inhibition process because of their low-cost, facile synthesis and highly abundant in the form of chemical or bio-waste or plant extracts [14–16]. In this process, molecules those are present in the inhibitors get strongly adsorbed, either by chemisorption or physisorption, at the surface of aluminium and its alloys and form a passive layer which in fact prevents the further corrosion against any aggressive media [3]. In particular, the best corrosion inhibitor/molecule must possess the constituent elements of N, C, H, O, S, Cl, Br and/or multiple bond(s) in their molecular structure [17–23]. Especially, the molecular structure and presence of lone electron pairs on heteroatoms are indeed an essential requisite to be a best inhibitor as it determines the adsorption on active sites of aluminium metal surfaces.

Due to ecological concern and environmental safeties, search for the low-cost, eco-friendly and green high-performance corrosion inhibitors, namely extracts of natural plants [24, 25], organic/inorganic compounds [26], Schiff bases [27, 28] and unused drugs/medicinal wastes [4, 29, 30], is of an important challenge in corrosion inhibitor-based research and in metallurgical industries. Generally, organic or bio-degradable polymer-based molecules are shown to have better adsorption behaviour, either physically and/or chemically on the active sites of aluminium surface and thereby create a protective layer that distinguishes out aluminium from its corrosive environment [3, 4, 31]. Among many corrosion inhibitors, Schiff base compounds were reported to be effective corrosion inhibitors for selected metals and alloys, such as aluminium [32–34] and mild steel [35–37], in acidic media due to their facile synthesis, eco-friendliness and their constituents. Interestingly, the presence of –C=N– group in Schiff bases significantly enhances their adsorption ability and thereby corrosion inhibition efficiency [38, 39]. Moreover, inhibitors based on Schiff bases get adsorbed effectively on the active sites of aluminium metal surface by the formation of coordinate covalent bond (chemical adsorption) or the electrostatic interaction between the metal and the inhibitor (physical adsorption) [40]. Moreover, the presence of more electron donating groups in the Schiff bases provides a strong adsorption at metal surfaces that makes them to be efficient inhibitor for aluminium and mild steel [41]. However, most of the recently reported Schiff-based organic ligands utilized as potential inhibitor for mild steel in the aggressive acid environments [42]. In particular, Chaitra et al. have recently shown that Schiff base of 3-(cyano-dimethylmethyl)-benzoic acid furan-2-ylmethylene-hydrazide performed as an efficient inhibitor with inhibition efficiency of 92% for mild steel corrosion in 0.5 M HCl solution [43]. Further, some of the Schiff based ligands, such as H: N^2,N^6-bis-(4-methylbenzylidene)pyridine-2,6-diamine [44], chitosan Schiff bases [45], 3-((4-hydroxy benzylidene)amino)-2-methylquinazolin-4(3H)-one [46], *N′*-(4-hydroxybenzylidene)nicotinic hydrazone [47], (4-((thiophene-2-ylmethylene)amino) benzamide) [48], have been recently proposed to be the best corrosion inhibitors for mild steel in HCl environments. However, there are very few reports, to the best of author's knowledge, were seen wherein Schiff bases have been utilized as high-performance corrosion inhibitor for aluminium corrosion against acidic media. In particular, Gomma et al. have been shown that Shiff base of aniline, *N*-(*p*-methoxybenzylidene) effectively adsorbs at the active sites of aluminium and prevents aluminium corrosion by forming the protective layer on top of it in the HCl medium [49].

Here, we have successfully synthesized two Schiff ligands, SB-1 [(4E)-*N*-((Z)-2-((furan-2-yl)methylimino) indolin-3-ylidene)(furan-2-yl)methanamine] and SB-2 [(7Z,8Z)-6-chloro-N2,N4-bis(1-(pyridin-2-yl)ethylidene) pyrimidine-2,4-diamine] and studied their corrosion inhibition ability for aluminium against aggressive H_2SO_4. Potentiodynamic polarization curves show that addition of Schiff bases in the acid solution shift the corrosion potential (E_{corr}) towards positive direction, suggesting that chosen SBs are performed as mixed-type inhbitiors. Electrochemical impedance studies reveal that the inhibition efficiency remarkably rises with increasing SBs concentration and the maximum inhibition efficiencies of 97% and – 95% were obtained for SB-1 and SB-2, respectively, for the inhibitor concentration of 500 ppm. Surface morphology studies further confirm that compounds of SB-1 and SB-2 have a strong tendency to adhere on top of aluminium and protects its corrosion against acidic media.

2 Experimental Methods

2.1 Synthesis of Schiff Base Compounds

Two Schiff base ligands, SB-1 [(4E)-*N*-((Z)-2-((furan-2-yl) methylimino) indolin-3-ylidene)(furan-2-yl)methanamine] and SB-2 [(7Z,8Z)-6-chloro-N2,N4-bis(1-(pyridin-2-yl)

ethylidene)pyrimidine-2,4-diamine] were synthesized and their inhibition performance against aluminium corrosion in acidic solution is also explored. A brief synthesis method of SB-1 and SB-2 has been discussed below.

SB-1 ligand was synthesized by refluxing the homogeneous mixtures of furfurylamine (0.005 mol) and isatin (0.0025 mol) in ethanol solution for 3 h. The product thus obtained as solid form was cooled down to room temperature, filtered, washed in ethanol and subsequently dried in the desiccators. SB-2 was prepared by refluxing method, where the homogenous mixtures of 2,6-diamino-4-chloropyrimidine and 2-acetyl pyridine were added in ethanol and the solution was refluxed for 2 h. The final product was cooled down to room temperature, washed in ethanol solution and dried out in the desiccators. The synthesized final products in solid form were used for inhibition of aluminium corrosion against acidic media.

These Schiff bases were characterized by infrared (IR) spectroscopy, UV–Visible and ^{1}H-NMR Spectra. The synthetic scheme for SB-(1 & 2) is shown in Fig. 1. The purity of the synthesized SB was determined by thin-layer chromatography using ethyl acetate/*n*-hexane (4:6) on the silica plate TLC plates aluminium (Al) silica.

2.2 Materials and Chemicals

Aluminium specimens with the purity of 98.5% were used for all corrosion-based experimental studies. The dimensions of used aluminium specimens were $2.5 \times 1.0 \times 0.2$ cm^3, wherein surface area of 1 cm^2 was exposed to the epoxy resin during electrochemical experiments. Before testing, aluminium coupons were finely polished using silicon carbide papers with the grade sizes range of 600–1200. The polished samples were properly rinsed and then degreased by using AR grade acetone. The aggressive test solution of 1 M H_2SO_4 solution was prepared by dilution of analytical grade with double distilled water.

2.3 Gravimetric Experiment

The weight loss of aluminium coupons in 1 M H_2SO_4 in the presence and absence of various concentrations of inhibitors

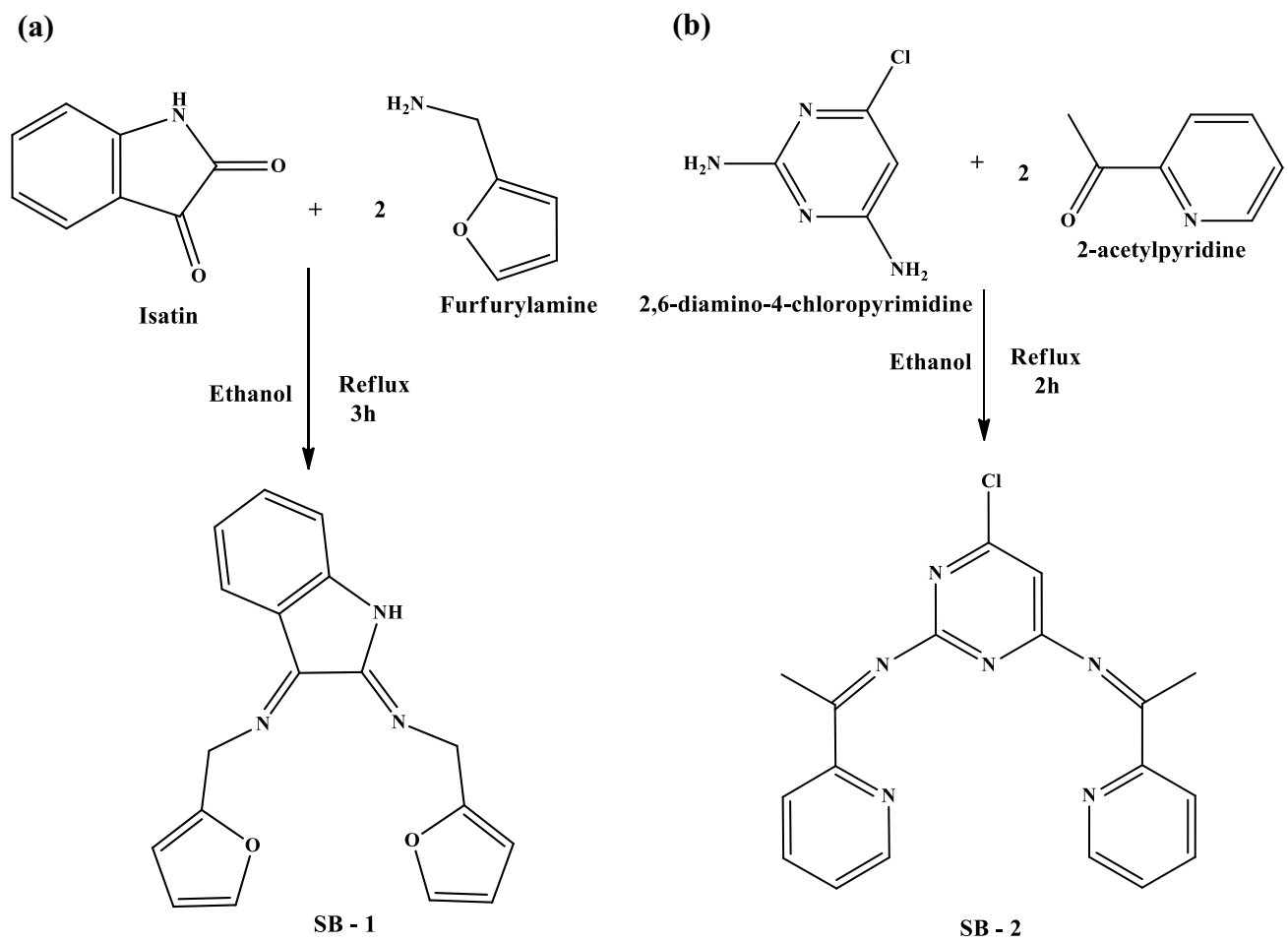

Fig. 1 The detailed reaction scheme of synthesis of Schiff base ligands, **a** SB-1 and **b** SB-2

is determined at different temperatures, ranging from 303 to 333 K in the absence and presence of SB-1 and SB-2 inhibitors after 3 h of immersion time. The corrosion rate was calculated using equation:

$$C_R = \frac{W}{At}, \tag{1}$$

where W is the mean value of weight loss of three parallel aluminium coupons, A is the total area of aluminium coupon and t is the immersion time (3 h). The percentage of inhibition efficiency ($\eta\%$) and surface coverage (θ) was calculated from the evaluated corrosion rates using following relation:

$$\eta\% = \frac{C_R - C_{R(i)}}{C_R} \times 100, \tag{2}$$

where W is the mean value of weight loss of three parallel aluminium coupons, A is the total area of a aluminium coupon and t is the immersion time (3 h). The percentage of inhibition efficiency ($\eta\%$) and surface coverage (θ) was calculated from the evaluated corrosion rates using following relation:

$$\theta = \frac{C_R - C_{R(i)}}{C_R}, \tag{3}$$

where C_R and $C_{R(i)}$ are corrosion rate (mg cm^{-2} h^{-1}) values of aluminium coupons in the absence and presence of inhibitors, respectively.

2.4 Electrochemical Experiment

Electrochemical measurements were performed by the method as described previously [50]. The electrochemical impedance measurements (EIS) were performed on aluminium specimens in the frequency range of 100 kHz to 0.01 Hz under potentiostatic conditions using an AC at open circuit potential with amplitude of 10 mV peak to peak. The charge transfer resistance was calculated from Nyquist plot from which corrosion inhibition efficiency was calculated using following equation:

$$\eta\% = \frac{R_{ct}^{i} - R_{ct}^{o}}{R_{ct}^{i}} \times 100, \tag{4}$$

where R_{ct}^{i} and R_{ct}^{o} charge transfer resistances in the presence and absence of SBs, respectively.

The potentiodynamic polarization studied was performed on aluminium specimens by automatically changing the electrode potential from −250 to +250 mV/SCE versus open circuit potential at a scan rate of 1 mV s^{-1}. The corrosion current density (i_{corr}) was calculated by extrapolating the linear segments of the cathodic and anodic Tafel slopes from which corrosion inhibition efficiency was calculated using the following equation:

$$\eta\% = \frac{i_{corr}^{\circ} - i_{corr}^{i}}{i_{corr}^{\circ}} \times 100, \tag{5}$$

where i_{corr}^{o} and i_{corr} are the corrosion current densities in the absence and presence of SBs.

2.5 Scanning Electron Microscope

Aluminium was immersed in 1 M H_2SO_4 solution in the absence and presence of optimum concentration of the SB for 3-h immersion time. Thereafter, aluminium specimens were taken out, washed with double distilled water, dried and finally analysed by SEM method. The SEM study was carried out using a Zeiss Evo 50XVP instrument at an accelerating voltage of 5 kV and ×500 magnification.

2.6 Study of Synergistic Effect

The synergistic effect of halide ions with the inhibitor on the corrosion inhibition was studied by potentiodynamic polarization studies. The synergism parameter was estimated using the following equation proposed by Aramki and Hackermann [51–53],

$$S_1 = \frac{1 - I_{1+2}}{1 - I'_{1+2}}, \tag{6}$$

where $I_{1+2} = (I_1 + I_2)$; I_1 is the inhibition efficiency of the halide, I_2, the inhibition efficiency of inhibitors and $I'_{(1+2)}$ the inhibition efficiency for SB-1 and SB-2 in combination with halide ion.

3 Results and Discussion

3.1 FT-IR Spectroscopy Analysis

FT-IR spectra of the Schiff base ligands of SB-1 and SB-2 are presented in Fig. 2. In the spectra, the observed sharp peaks at 3181 and 3317 cm^{-1} represent the presence of N–H group. From Fig. 2, it is seen that the azomethine group has the medium intensity weak bands at 1613 and 1642 cm^{-1}. Moreover, the second strong bands at 1151 and 1272 cm^{-1} are responsible for C–N group. In addition, the band appears at 1192 cm^{-1} in the IR spectrum of the SB-1 which belongs to C–O stretching vibrations of the furfurylamine [54]. Thus, presence of these functional groups in the Schiff bases form a protective layer at aluminium surface and thereby enhance the anti-corrosion. In particular, the adsorption active elements of O, N, C, H and functional groups of N–H, C–N,

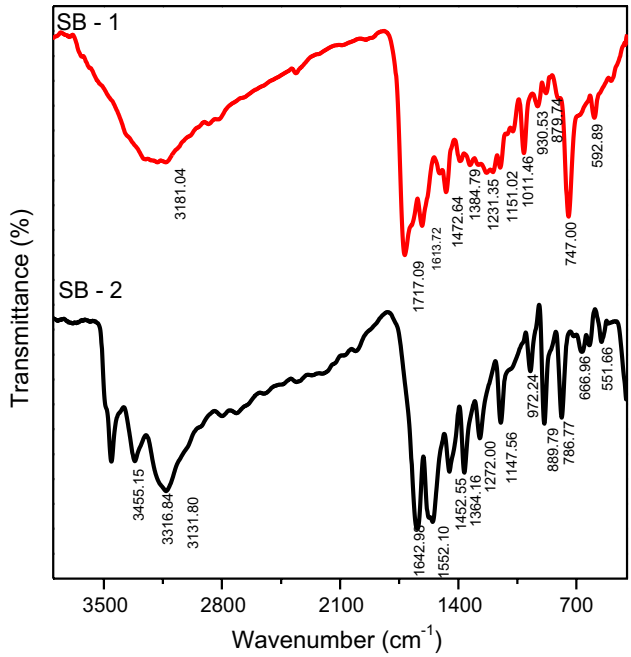

Fig. 2 FT-IR spectra of as-synthesized Schiff bases, SB-1 and SB-2

C–O in SB-1 and SB-2 are expected to strongly adhere to aluminium surface and protect its corrosion against aggressive acidic media.

3.2 UV Spectroscopy Analysis

The typical UV–Vis spectra of the Schiff bases of SB-1 and SB-2 are shown in Fig. 3a, b, respectively. Both the ligands show almost similar peaks with one sharp and one broad band observed in the regions of 223–247 nm and 333–342 nm, respectively. The presence of HC=N– group in the inhibitors exhibits sharp peaks on the higher energy range of 223–247 nm, which is due to the excitation of the π–π* transitions in the aromatic system. The spectral band at 333–342 nm is appeared due to N–H group n → π* transition [55, 56].

3.3 ^{1}H-NMR Spectral Analysis

The structure and purity of the synthesized ligands of SB-1 and SB-2 were confirmed by ^{1}H-NMR Spectra. Figure 4a, b shows ^{1}H-NMR spectra of inhibitors of SB-1 and SB-2, respectively. From both the spectra, the multiplets obtained at 7.1–7.6 and 6.3–6.5 ppm are attributed to the aromatic protons. Moreover, peak at 8.1 ppm in SB-2 shows the presence of heterocyclic NH proton and a singlet obtained at 9.6 ppm indicates the formation of imine (–HC=N). In the ^{1}H-NMR Spectra of the SB-2, a peak obtained at 3.3 ppm is due to the presence of methyl protons [57].

3.4 Weight Loss Studies

3.4.1 Effect of SBs on Corrosion Rate

The corrosion rate (C_r) of aluminium in 1 M H_2SO_4 solution in the absence and presence of newly synthesized SB concentration at different temperatures was estimated using a conventional weight loss method [3, 4]. Figure 5a, b illustrates the corrosion rate of aluminium as the function of inhibitors concentration of SB-1 and SB-2, respectively, at temperature range of 303–333 K. From the results, it is clearly seen that corrosion rate rapidly increases with temperature and it substantially decreases with addition of SB concentrations. In the absence of inhibitors, the corrosion rate of aluminium in 1 M H_2SO_4 is estimated to be 2.59 mg cm^{-2} h^{-1} at 303 K which further increases with temperature and reaches 3.77 mg cm^{-2} h^{-1} at 333 K as increase in temperature induces the corrosion reaction of aggressive H_2SO_4 solution and surface of aluminium metal.

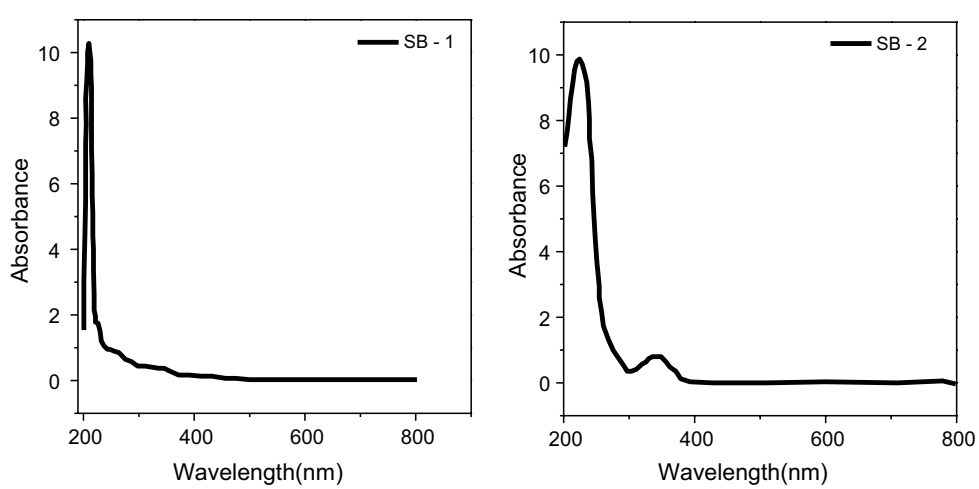

Fig. 3 UV–Vis spectra of as-synthesized Schiff bases, SB-1 and SB-2

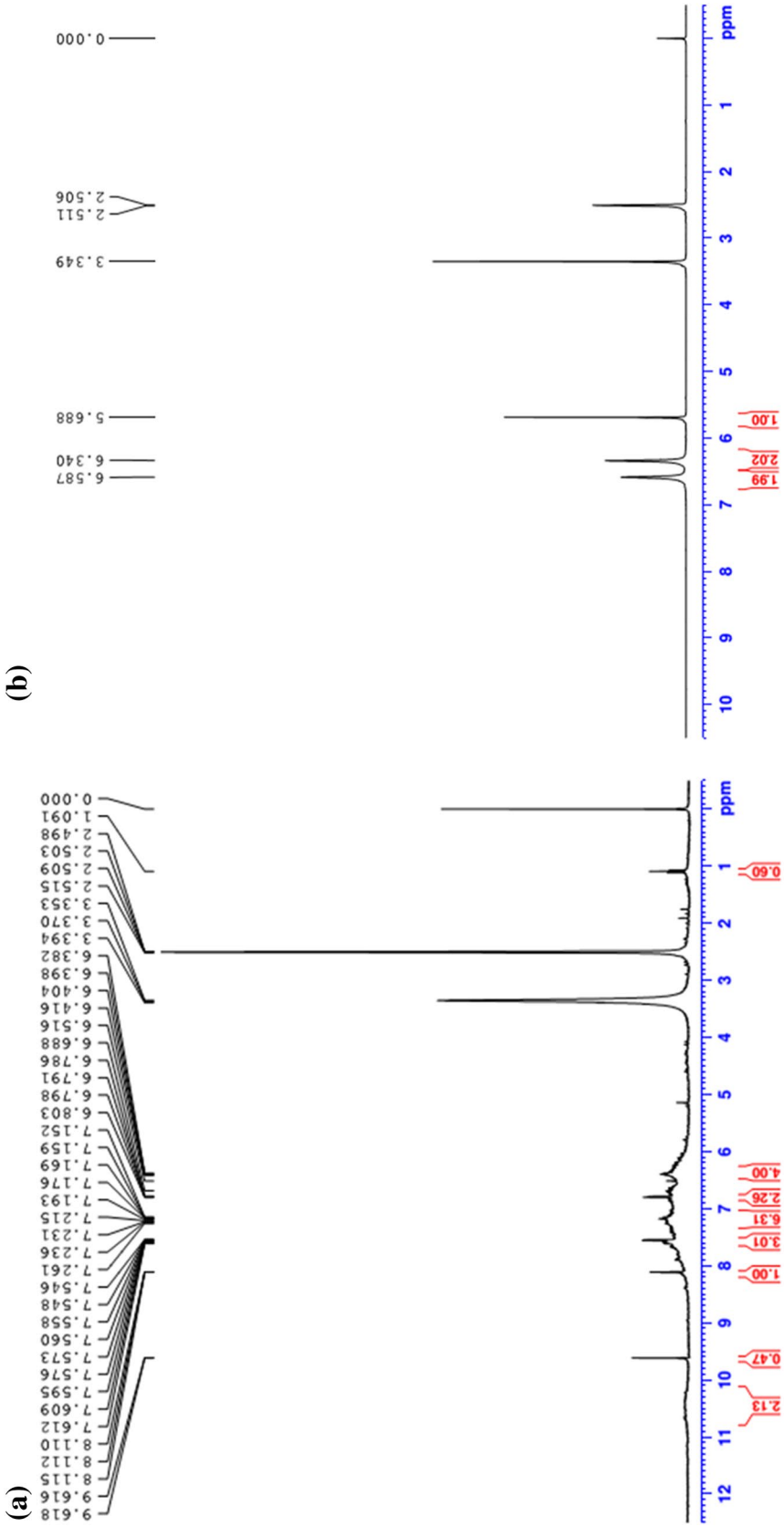

Fig. 4 ^{1}H NMR spectra of as-synthesized Schiff bases, **a** SB-1 and **b** SB-2

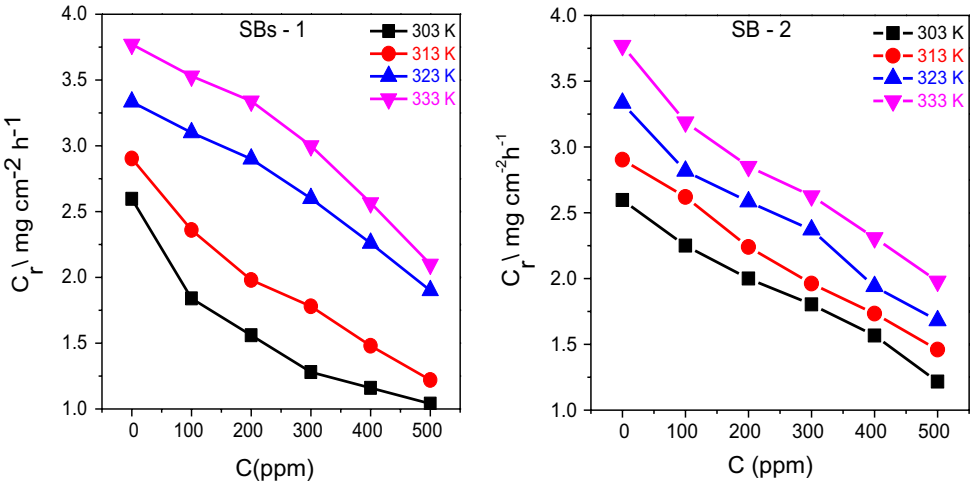

Fig. 5 Plot of corrosion rate (C_r) of aluminium corrosion versus inhibition (Schiff bases) concentration in 1 M H_2SO_4 at room temperature

In the presence of 500 ppm inhibitor, the corrosion rate of aluminium is drastically reduced to 1.21 mg cm^{-2} h^{-1} and 1.04 mg cm^{-1} h^{-1} for the as-synthesized Schiff bases of SB-1 and SB-2, respectively. Further, the reduction in C_r upon addition of SBs concentration is due to the increase in adsorption coverage that in fact protects aluminium metal from the aggressive acidic medium by forming the protective or inhibition layer on top of aluminium surface. At any given inhibitor concentration, the corrosion rate (C_r) of aluminium is decreased by the addition of SB-1 than SB-2 (see Fig. 5a, b), which indicates that SB-1 exhibits better inhibitive performance than that of SB-2 which is often decided by the molecules or functional groups those present in the inhibitors and get adsorbed at active sites of aluminium metal. Table 1 summarizes the effects of solution temperature and inhibitor concentration of SB-1 and SB-2 on corrosion rate (C_r).

3.4.2 Effect of SBs on Inhibition Efficiency

Figure 6 represents inhibition efficiency (I.E%) values obtained from the weight loss method for aluminium corrosion in 1 M H_2SO_4 solution in the presence of various concentrations of as-synthesized SB-1 and SB-2 at room temperature. From Fig. 6a, b, it is seen that the inhibition efficiency increases with increase in the Schiff bases concentration. At 500 ppm, the maximum inhibition efficiency is 97.62% for SB-1 and 94.02% for SB-2, which illustrates that both the Schiff bases act as efficient corrosion inhibitors for aluminium in 1 M H_2SO_4 and SB-1 shows slightly higher inhibition potential than SB-2. The increase in I.E% with rise SBs concentration is due to the increase in the surface coverage of Schiff bases on aluminium surface that protects the further corrosion. The reason behind the huge enhancement in the inhibition efficiency is higher inhibitive performance of isatin and –C_5H_5N than amino, azomethine

Table 1 Temperature effect on aluminium corrosion rate and corrosion inhibition efficiency in 1 M H_2SO_4 with different concentrations of SB-1 and SB-2

Inhibitor	Concentration (ppm)	Temperature							
		303 K	313 K	323 K	333 K	303 K	313 K	323 K	333 K
		Corrosion rate (mg cm^{-2} h^{-1})				Inhibition efficiency (I.E%)			
SB-1	Blank	2.59	2.9	3.33	3.77	–	–	–	–
	100	1.84	2.36	3.1	3.53	86.87	84.4	83.27	78.86
	200	1.56	1.98	2.9	3.34	87.34	86.66	83.85	81.77
	300	1.28	1.78	2.6	3	90.64	88.32	84.94	83.96
	400	1.16	1.48	2.26	2.56	94.98	89.67	88.66	86.08
	500	1.04	1.22	1.9	2.1	97.68	90.29	89.65	86.88
SB-2	100	2.25	2.62	2.81	3.19	81.36	80.16	78.94	76.98
	200	2	2.24	2.58	2.85	83.35	82.36	81.05	80.32
	300	1.8	1.96	2.37	2.62	86.33	85.04	84	83.16
	400	1.56	1.73	1.94	2.31	91.03	87.56	86.05	85.49
	500	1.21	1.46	1.68	1.98	94.02	89.74	87.94	86.12

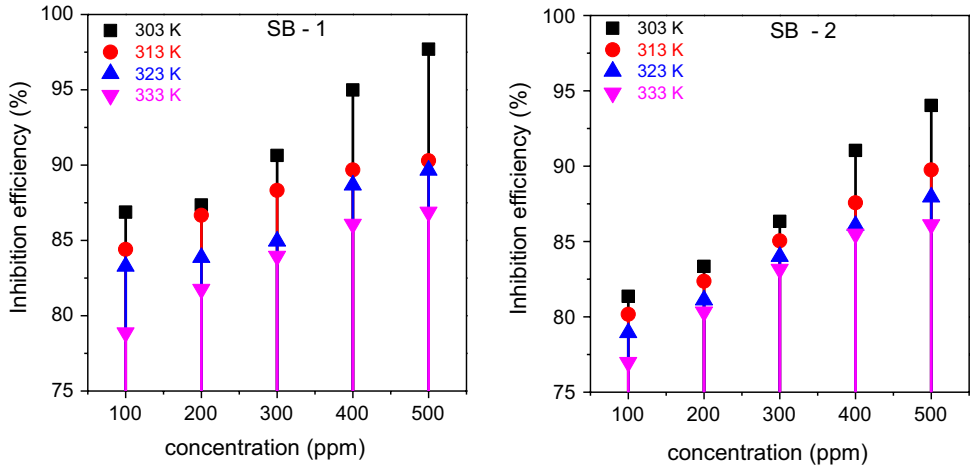

Fig. 6 Inhibition efficiency of aluminium corrosion versus concentration of as-synthesized Schiff bases of SB-1 and SB-2 in 1 M H_2SO_4 at room temperature

group and furfurylamine. Moreover, SB-1 shows better inhibition efficiency than that of SB-2 which is due to the strong conjugation between isatin and pyrimidine ring that significantly facilitates the adsorption of the furfurylamine and acetyl group thereby efficiently covering more surface area than the adsorption of amino, azomethine group and C–N group of aluminium surface.

3.4.3 Adsorption Isotherm Studies

The adsorption isotherm is an essential tool in understanding the mechanism of interaction between metal surface and the inhibitor [58]. Our experimental results were fitted with several adsorption isotherms such as Langmuir Temkin, and Freundlich isotherms [3, 4, 58], among which Langmuir isotherm has shown the best fit with regression coefficient (R^2) values close to unity. Figure 7 shows the Langmuir isotherm plots which provide a linear response (straight line) between log ($\theta/1-\theta$) and $C_{(inh)}$. To understand the interaction between synthesized inhibitor and metal surface of aluminium, the constant value for adsorption–desorption process, K_{ads} was calculated using the standard free energy of adsorption (ΔG^0_{ads}) relation [3, 4] and its vales are given in Table 2. The calculated values of ΔG^0_{ads} are given in Table 2. It is clearly seen that the value of ΔG^0_{ads} for as-synthesized Schiff bases (SB-1 and SB-2) lies in the range −29.52 to −38.21 kJ mol^{-1}; negative sign of ΔG^0_{ads} depicts that prepared Schiff bases automatically get attracted by the active regions of aluminium that leads to protective layer formation [3]. Moreover, the estimated values of ΔG^0_{ads} are in between the threshold values of physical and chemical adsorption, stating that as-synthesized molecules of Schiff bases (SB-1 and SB-2) possess both physisorption and chemisorption at aluminium surface in the presence of 1 M H_2SO_4 solution [30, 59].

3.4.4 Effect of Temperature

To evaluate the effect of temperature on the inhibition efficiency, the weight loss experiments were performed in the temperature range of 303–333 K. The variation of corrosion rate (C_r) with temperature is represented in Table 1.

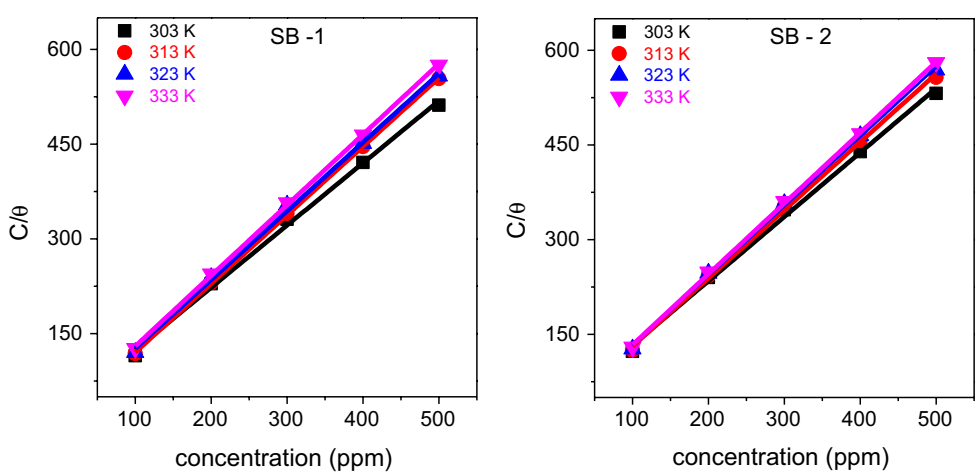

Fig. 7 Langmuir isotherm adsorption plots for aluminium corrosion in 1 M H_2SO_4 containing different concentrations of as-synthesized Schiff bases, **a** SB-1 and **b** SB-2 at room temperature

Table 2 Adsorption parameters derived from Langmuir adsorption isotherms for aluminium corrosion in 1 M H_2SO_4 at different temperatures

Temperature (K)	K_{ads} (kJ mol^{-1})		ΔG^{o}_{ads} (kJ mol^{-1})	
	SB-1	SBs-2	SB-1	SB-2
303	8.70	17.24	−29.52	−36.96
313	7.32	10.21	−30.92	−37.16
323	5.39	7.39	−31.22	−38.22
333	4.78	5.50	−32.32	−38.21

From the results, it can be observed that I.E% decreases with increasing temperature associated with the desorption of the adsorbed Schiff bases (SB-1 and SB-2) molecules from aluminium surface and leading to reduction in I.E%. The effect of temperature on corrosion rate can be effectively estimated by Arrhenius equation.

Arrhenius plots of log C_r versus $1/T$ of aluminium in 1 M H_2SO_4 solution are shown in Fig. 8, which shows a linear response. The values of activation energy, E_a were calculated from the slope and the corresponding values are listed in Table 3. The tabulated data revealed that values of E_a for inhibited solution are greater than that of uninhibited solution. These enhancements in E_a in the presence of Schiff bases (SB-1 and SB-2) confirm the formation of higher energy barrier for corrosion process to happen, suggesting that adsorbed SBs form a passive film on aluminium surface and prevents the charge/mass transfer reaction that usually occurs on the surface [60]. Moreover, the increased value of E_a also suggests that rate of aluminium dissolution significantly suppressed with addition of SBs ligands due to the formation of metal-inhibitor complex at the surface of aluminium [61]. From the activation energy, thermodynamic parameters (ΔH°_{ads} and ΔS°_{ads}) were calculated and listed in Fig. 9 and Table 3. The positive values of ΔH°_{ads} both in the absence and presence of SBs reflect the endothermic nature of aluminium dissolution process [62, 63]. The negative values of entropy of activation both in the absence and presence of inhibitor imply that the activated complex in the rate determining step represents an association rather than a dissociation step, meaning that a decrease in disordering takes place on going from reactants to the activated complex [64–66].

3.4.5 Polarization Study

The Tafel polarization curves obtained for aluminium in 1 M H_2SO_4 absence and presence of as-synthesized Schiff bases (SB-1 and SB-2) at various concentrations are shown in Fig. 10. Further, Table 4 represents the derived polarization

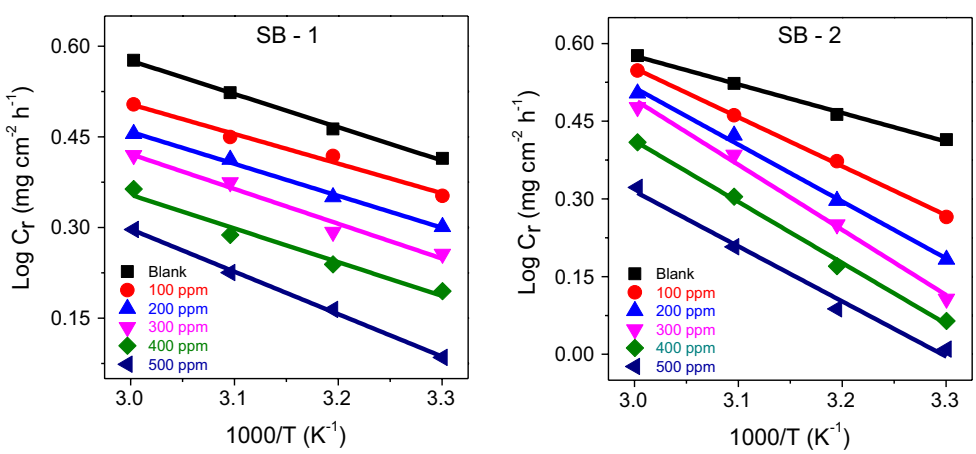

Fig. 8 Arrhenius plots for aluminium corrosion in 1 M H_2SO_4 in the absence and presence of different concentrations of as-synthesized Schiff bases (SB-1 and SB-2)

Table 3 Activation parameters for aluminium corrosion in 1 M H_2SO_4 in the absence and presence of different concentrations of SB

Concentration (ppm)	E_a (kJ mol^{-1})		ΔH°_{ads} (kJ mol^{-1})		ΔS°_{ads} (J mol^{-1}K^{-1})	
	SB-1	SB-2	SB-1	SB-2	SB-1	SB-2
Blank	34.14	34.14	67.62	67.62	186.10	186.10
100	41.56	51.24	74.92	70.25	187.18	175.36
200	43.87	54.53	79.11	73.59	187.45	186.60
300	45.81	58.17	80.42	78.44	190.00	195.72
400	48.23	71.29	83.97	84.21	190.90	196.83
500	50.99	74.79	94.22	88.40	194.34	203.90

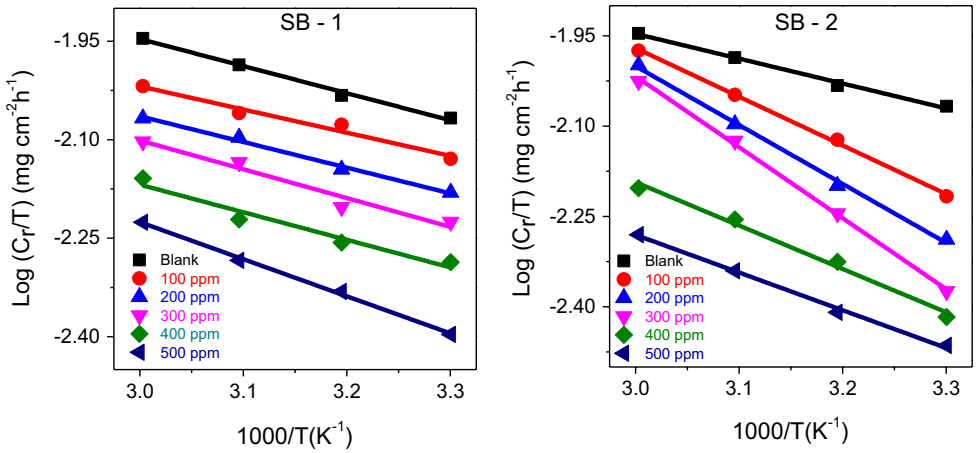

Fig. 9 Transition state plots for aluminium corrosion in 1 M H_2SO_4 in the absence and presence of different concentrations of as-synthesized Schiff bases (SB-1 and SB-2)

parameters, i.e. corrosion potential (E_{corr}), cathodic (β_c) and anodic (β_a) Tafel slopes, corrosion current density (I_{corr}), surface coverage (θ) and the inhibition efficiency (%) for aluminium corrosion with and without SB ligands inhibitor. From Fig. 10 and Table 4, it is clear that addition of Schiff bases in 1 M H_2SO_4 solution shifts the corrosion potential (E_{corr}) towards positive direction that illustrates that chosen Schiff bases (SB-1 and SB-2) are efficient corrosion inhibitors and performed as mixed-type inhibitors [67]. Interestingly, the presence of SB-1 and SB-2 in acidic solution additionally causes a significant reduction in the corrosion current, (I_{corr}). In particular, the estimated corrosion current (I_{corr}) for blank is – 419.7 μA cm^{-2}, which is rapidly reduced to – 17 and – 24 μA cm^{-2} by addition of SB-1 and SB-2 for the concentration of 500 ppm, respectively.

Moreover, the presence of SBs ligands in 1 M H_2SO_4 solution predominantly pushes the cathodic curves towards lower current densities. On the other hand, the anodic reaction is also slightly affected by the addition of inhibitors, which can be visualized from the reduction in anodic Tofel slope (β_a). A clear inspection of Fig. 10 reveals that both anodic dissolution of aluminium and cathodic hydrogen evolution reaction are effectively inhibited with the addition of Schiff bases to the acid solution.

Moreover, the inhibition of these reactions is more pronounced with the increasing inhibitors concentration. As known, the inhibition efficiency is also associated with a shift in both cathodic and anodic branches of the polarization curves towards lower current densities. From Table 4, It is shown that inhibition efficiency (I.E%) significantly increases with addition of SBs inhibitors and it reaches the maximum inhibition efficiency of 97% for SB-1 and 94% for SB-2 at the concentration for 500 ppm. Generally, the functional groups and structure of the inhibitors play predominant role during the adsorption process [68]. The presence of functional groups of N–H, C–N, C–O and aromatic rings in SB-1 and SB-2 get adsorbed on the active sites of aluminium, and effectively controls the anodic and cathodic reactions during corrosion process, which altogether protect aluminium corrosion against aggressive acidic media. The inhibition efficiency values determined using potentiodynamic polarization curves are in good

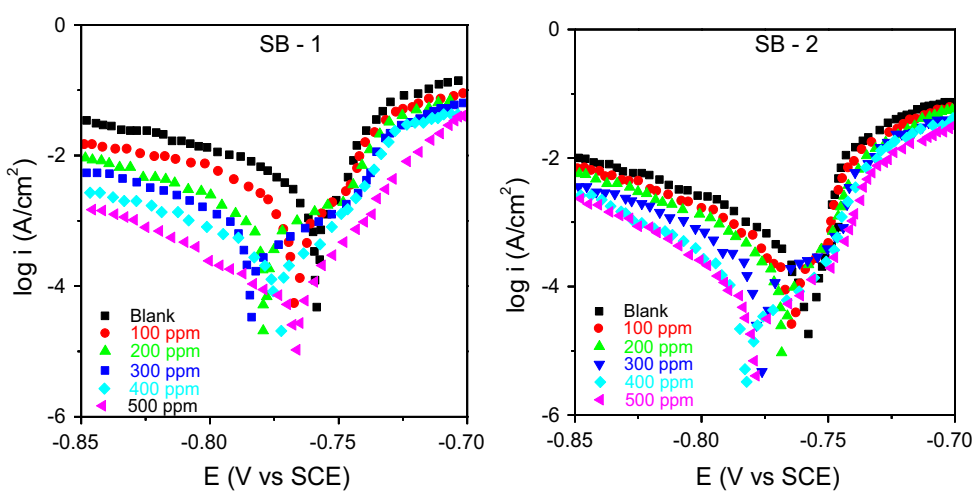

Fig. 10 Potentiodynamic polarization curves for aluminium corrosion in 1 M H_2SO_4 containing different concentrations of as-synthesized Schiff bases (SB-1 and SB-2)

Table 4 Corrosion parameters obtained from potentiodynamic polarization curves for corrosion of aluminium in 1 M H_2SO_4 with different concentrations of SB-1 and SB-2 at room temperature

Inhibitor	Concentration (ppm)	E_{corr} (mV vs. SCE)	I_{corr} (μA/cm^{-2})	β_a (mV/dec^{-1})	I.E (%)
	Blank	−769	419.7	96	–
SB-1	100	−771	106	18.03	74.74
	200	−779	89	19.17	83.79
	300	−783	71	19.17	88.08
	400	−772	28	18.0	92.18
	500	−766	17	16.8	97.02
SB-2	100	−770	117	17.30	72.12
	200	−772	92	17.94	78.07
	300	−779	75	16.15	82.13
	400	−782	48	15.96	88.56
	500	−780	24	14.02	94.28

agreement with EIS measurements, discussed in the later section.

3.5 Electrochemical Impedance Spectroscopic Study

Figure 11 represents the Nyquist plots for aluminium corrosion in 1 M H_2SO_4 solution in the absence and presence of different concentration of the as-synthesized Schiff bases of SB-1 and SB-2. Figure 11 states that all the Nyquist plots show same trend for blank and inhibitor added ones, suggesting that chosen Schiff bases strongly inhibit aluminium corrosion without affecting the corrosion mechanism [69]. Further, it is clearly seen that Nyquist plots consist of a depressed semicircle at high frequency region which is indeed typical characteristic features that any solid metal electrodes encounter during the corrosion process [3, 69]. The formation of semicircle suggests that aluminium corrosion in acidic media is mainly controlled by the charge transfer resistance and the presence of protective layer on top of aluminium surface [3, 70]. Additionally, the diameter of semicircle increases with the increase in inhibitor concentration which indicates the inhibitor molecules strongly adsorb on the metal surface and protects aluminium from further corrosion.

Impedance parameters, such as R_{ct}, C_{dl} and I.E%, were derived from Nyquist plots by employing an equivalent circuit and their values are listed in Table 5. The results show that the addition of SBs causes significant increase in the R_{ct} value, suggesting that the presence of SB impedes the charge transfer reaction and corrosion that occurr on aluminium surface by forming protective film on the surface [71].

From the results, it is also clear that values of C_{dl} drastically decrease in the presence of SBs. In particular, the C_{dl} value decreases from 115 to 5.9 μF cm^{-2} and 6.3 μF cm^{-2} for SB-1 and SB-2, respectively, in the concentration of 500 ppm. This reduction in C_{dl} is due to the decrease in local dielectric constant and/or an increase in the thickness of the electrical double layer, occurring because of the adsorption of the molecules of Schiff bases that adhere on the surface. From this EIS study, it is noteworthy to say that adsorption mechanism is majorly contributing to the

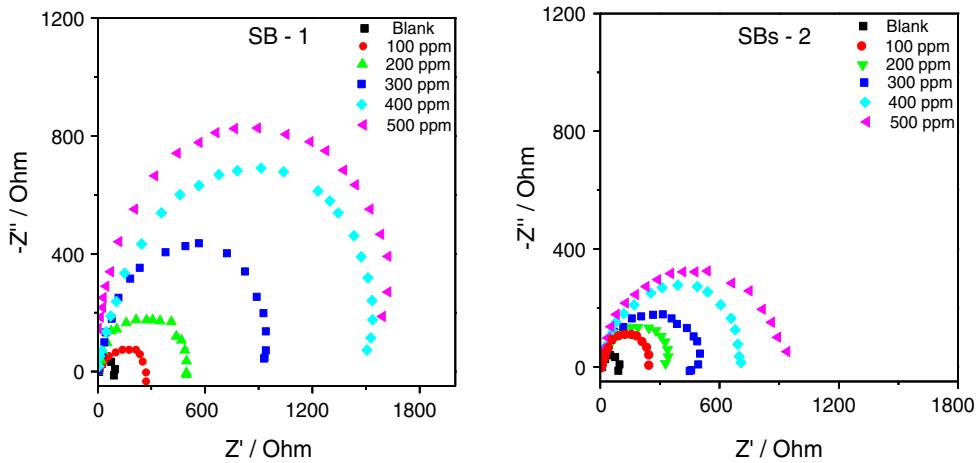

Fig. 11 Nyquist plots for aluminium corrosion in 1 M H_2SO_4 solution in the absence and presence of different concentration of as-synthesized Schiff bases (SB-1 and SB-2)

Table 5 Impedance parameters for corrosion of aluminium in 1 M H_2SO_4 with different concentrations of SB-1 and SB-2 at room temperature

Inhibitor	Concentration (ppm)	R_{ct} (Ω cm^2)	C_{dl} (μF cm^{-2})	I.E (%)
	Blank	58.5	115	–
SB-1	100	262.7	31.1	77.73
	200	492.3	16.7	88.11
	300	968.8	8.5	93.96
	400	1514	5.9	96.13
	500	1600	5.9	97.34
SB-2	100	233.4	30.8	74.93
	200	314.7	24.3	81.41
	300	426.2	19.2	86.27
	400	783.4	12.6	92.53
	500	1093.2	6.3	94.64

inhibition of aluminium corrosion upon addition of SBs [50]. In addition, Table 5 further illustrates that the inhibition efficiency remarkably rises with increasing SBs concentration and the maximum inhibition efficiencies of 97% and – 95% were obtained for SB-1 and SB-2, respectively, for the inhibitor concentration of 500 ppm. These results further have good agreement with weight loss method and potentiodynamic polarization curves.

3.6 Scanning Electron Microscope

The surface morphologies and microstructures of blank and inhibited aluminium samples were studied using scanning electron microscope (SEM). Figure 12a–d illustrates the SEM micrographs of aluminium specimens with and without the presence of SBs ligands in acidic medium of 1 M H_2SO_4. Figure 12a, b depicts the micrographs of aluminium before and after immersion of aluminium in 1 M H_2SO_4 solution, respectively. Surface morphology of aluminium dipped into aggressive acid in the absence of SBs shows notably rough corroded surface with deep and denser pits due to aggressive corrosion behaviour of 1 M H_2SO_4. However, the presence of SB ligands in 1 M H_2SO_4 solution remarkably reduces the deep pits and corrosion of aluminium as seen in the micrographs of Fig. 12c, d. A reason behind the huge inhibition of aluminium corrosion is addition of SBs ligands in the acidic solution gets adsorbed on the active sites of aluminium and forms a thin passive layer thereby preventing aluminium from its dissolution caused by 1 M H_2SO_4. From these micrographs one could conclude that compounds of SB-1 and SB-2 have a strong tendency to adhere on top of aluminium and protects its corrosion against acidic media.

3.7 Synergism Studies

The synergistic effect of halide ions on the corrosion inhibition along with inhibitors of SB-1 and SB-2 was extensively studied by weight loss studies. Synergistic effect is generally represented as an effective method to increase the inhibitive nature of the given inhibitors, to reduce the quantity of usage, and to diversify the application of inhibitor in the chosen corrosive media. Typically, the synergistic influence of halide ions on the inhibitive effect of inhibitor was significantly studied by adding potassium halides (KX) to the test solutions by which the role of halide ions with inhibitor on adsorption process of metal surface could be estimated. In this view, the strength of the synergistic effect can be evaluated by the synergism parameter (S) using Aramaki and Hackman relationship. In this context, the value of $S < 1$ implies antagonistic behaviour and occurrence of competitive adsorption, whereas $S > 1$ indicates a synergistic effect [63]. Halides have been reported to increase the inhibition efficiency of metal corrosion along with given strong acids. In particular, the inhibitive effect of halides increases in the order of $Cl^- < Br^- < I^-$. Table 6 provides the synergistic effect of halide ion with SB-1 and SB-2 due to cooperative adsorption of halide ion and the inhibitor. In most cases, the halide ions are anticipated to chemisorption on the surface and utilized inhibitor molecules are ascribed to adsorb on adsorbed halide layers. This behaviour of KI and organic inhibitors was also reported by other researchers [52, 53, 72].

The values of S as presented in Table 6 are greater than unity which clearly represents that the enhanced inhibition efficiency by addition of SB ligands in combination with halides is mainly due to synergistic effect. This enhancement in inhibition efficiency can be explained on the basis that halide has a great tendency to get adsorbed on aluminium surface by strong chemisorptions and cations of inhibitor molecules then attach on layer of halide ions by columbic attraction. These adsorbed halide ions with cations of the inhibitor create more surface coverage and by which it protects aluminium corrosion against aggressive acids. Additionally, the greater influence of iodide halide (I^-) compared to other halide ions of Cl^- and Br^-over SBs at room temperature may be attributed to its large ionic radius, high hydrophobicity and low electronegativity.

4 Conclusion

We have successfully synthesized two novel Schiff bases and demonstrated their inhibition ability upon aluminium corrosion in 1 M H_2SO_4 solution using electrochemical and non-electrochemical methods. It was shown that addition of Schiff bases substantially increased the corrosion inhibition

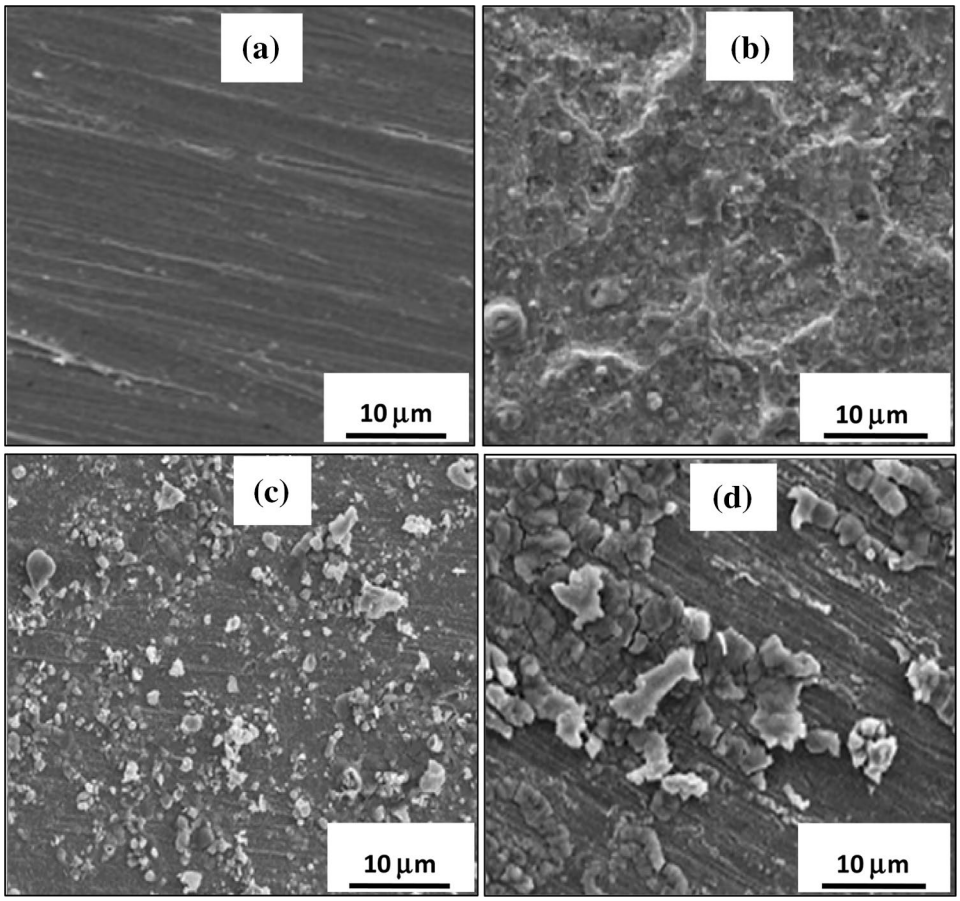

Fig. 12 **a**–**d** SEM micrographs of aluminium surface after 3-h immersion **a** aluminium **b** in 1 M H_2SO_4 without SB **c** in 1 M H_2SO_4 with SB-1 **d** in 1 M H_2SO_4 with SB-2

Table 6 Synergism parameter (*S*) for 400 ppm SB in combination with 100 ppm KCl, KBr, KI

Medium	Inhibitor	Concentration (ppm)	Synergism parameter (*S*)
1 M H_2SO_4	SB-1	Inhibitor + 100 ppm KCl	0.82
		Inhibitor + 100 ppm KBr	0.94
		Inhibitor + 100 ppm KI	1.25
	SB-2	Inhibitor + 100 ppm KCl	0.89
		Inhibitor + 100 ppm KBr	0.98
		Inhibitor + 100 ppm KI	1.68

efficiency. Further, potentiodynamic polarization curves revealed that chosen Schiff bases performed as mixed-type inhibitors. Additionally, electrochemical impedance studies (EIS) were also shown that the inhibition efficiency, I.E%, remarkably increased with increasing SBs concentration and thus the maximum inhibition efficiencies of 97% and −95% were obtained for SB-1 and SB-2, respectively, for the inhibitor concentration of 500 ppm. Adsorption process obeyed Langmuir adsorption isotherm and regarded as both physical and chemical adsorption. SEM micrographs of inhibited samples showed that compounds of SB-1 and SB-2 have extremely high tendency to adhere on active sites of aluminium and protect its corrosion against acidic media.

References

1. Fouda AS, Al-Sarawy AA, Ahmed FS, El-Abbasy HM (2009) Corrosion inhibition of aluminium 6063 using some pharmaceutical compounds. Corros Sci 51:485–492
2. Nathiya RS, Raj V (2017) Evaluation of *Dryopteris cochleata* leaf extracts as green inhibitor for corrosion of aluminium in 1 M H_2SO_4. Egypt J Pet 26:313–323
3. Nathiya RS, Suresh P, Murugesan V, Anbarasan PM, Raj V (2017) Agarose as an efficient inhibitor for aluminium corrosion in acidic medium: an experimental and theoretical study. J Bio Tribo Corros 3:44
4. Nathiya RS, Perumal S, Murugesan V, Raj V (2018) Expired drugs: environmentally safe inhibitors for aluminium corrosion in 1 M H_2SO_4. J Bio Tribo Corros 4:4
5. Abiola OK, Otaigbe JOE (2008) Effect of common water contaminants on the corrosion of aluminium alloys in ethylene glycol–water solution. Corros Sci 50:242–247
6. He X, Jiang Y, Li C, Wang W, Hou B, Wu L (2014) Inhibition properties and adsorption behavior of imidazole and 2-phenyl-2-imidazoline on AA5052 in 1.0 M HCl solution. Corros Sci 83:124–136
7. El Nemr A, Moneer AA, Khaled A, El Sikaily A, El-Said GF (2014) Modeling of synergistic halide additives' effect on the

corrosion of aluminum in basic solution containing dye. Mater Chem Phys 144:139–154
8. Wang D, Li H, Liu J, Zhang D, Gao L, Tong L (2015) Evaluation of AA5052 alloy anode in alkaline electrolyte with organic rare-earth complex additives for aluminium-air batteries. J Power Sour 293:484–491
9. Zhu Y, Free ML, Yi G (2015) Electrochemical measurement, modeling, and prediction of corrosion inhibition efficiency of ternary mixtures of homologous surfactants in salt solution. Corros Sci 98:417–429
10. Abiola OK, Otaigbe JOE, Kio OJ (2009) *Gossipium hirsutum* L. extracts as green corrosion inhibitor for aluminum in NaOH solution. Corros Sci 51:1879–1881
11. Mercier D, Barthés-Labrousse MG (2009) The role of chelating agents on the corrosion mechanisms of aluminium in alkaline aqueous solutions. Corros Sci 51:339–348
12. Zhang J, Klasky M, Letellier BC (2009) Schiff bases of increasing complexity as mild steel corrosion inhibitors in 2 M HCl. J Nucl Mater 384:175–189
13. Shao HB, Wang JM, Zhang Z, Zhang JQ, Cao CN (2003) The cooperative effect of calcium ions and tartrate ions on the corrosion inhibition of pure aluminum in an alkaline solution. Mater Chem Phys 77:305–309
14. Lashgari M, Arshadi MR, Miandari S (2010) The enhancing power of iodide on corrosion prevention of mild steel in the presence of a synthetic-soluble Schiff base: electrochemical and surface analyses. Electrochim Acta 55:6058–6063
15. Küstü C, Emregül KC, Atakol O (2007) Schiff bases of increasing complexity as mild steel corrosion inhibitors in 2 M HCl. Corros Sci 49:2800–2814
16. Nathiya RS, Perumal S, Murugesan V, Raj V (2019) Evaluation of extracts of *Borassus flabellifer* dust as green inhibitors for aluminium corrosion in acidic media. Mater Sci Semicond Process 104:104674
17. Yıldız R (2015) An electrochemical and theoretical evaluation of 4,6-diamino-2-pyrimidinethiolas a corrosion inhibitor for mild steel in HCl solutions. Corros Sci 90:544–553
18. Zeng RC, Liu ZG, Zhang F, Li SQ, Cui HZ, Han EH (2014) Corrosion of molybdate intercalated hydrotalcite coating on AZ31 Mg alloy. J Mater Chem A 2:13049–13057
19. Obot IB, Ebenso EE, Kabanda MM (2013) Metronidazole as environmentally safe corrosion inhibitor for mild steel in 0.5 M HCl: experimental and theoretical investigation. J Environ Chem Eng 1:431–439
20. Finšgar M, Jackson J (2014) Application of corrosion inhibitors for steels in acidic media for the oil and gas industry: a review. Corros Sci 86:17–41
21. Mazumder MAJ, Al-Muallem HA, Faiz M, Ali SA (2014) Design and synthesis of a novel class of inhibitors for mild steel corrosion in acidic and carbon dioxide-saturated saline media. Corros Sci 87:187–198
22. Aytaç A, Özmen U, Kabasakaloğlu M (2005) Investigation of some Schiff bases as acidic corrosion of alloy AA3102. Mater Chem Phys 89:176–181
23. Li X, Deng S, Fu H, Xie X (2014) Synergistic inhibition effects of bamboo leaf extract/major components and iodide ion on the corrosion of steel in H_3PO_4 solution. Corros Sci 78:29–42
24. Oguzie EE, Oguzie KL, Akalezi CO, Udeze IO, Ogbulie JN, Njoku VO (2013) Natural products for materials protection: corrosion and microbial growth inhibition using *Capsicum frutescens* biomass extracts. ACS Sustain Chem Eng 2:214–225
25. Xhanari K, Finšgarv M, Hrnčič MK, Maver U, Knez Ž, Seiti B (2017) Green corrosion inhibitors for aluminium and its alloys: a review. RSC Adv 7:27299–27330
26. Xhanari K, Finšgar M (2016) Organic corrosion inhibitors for aluminium and its alloys in acid solutions: a review. RSC Adv 6:62833–62857
27. Safak S, Duran B, Yurt A, Türkoglu G (2012) Schiff bases as corrosion inhibitor for aluminium in HCl solution. Corros Sci 54:251–259
28. Gupta NK, Quraishi MA, Vermaa C, Mukherjee AK (2016) Green Schiff's bases as corrosion inhibitors for mild steel in 1 M HCl solution: experimental and theoretical approach. RSC Adv 6:102076–102087
29. Gupta NK, Gopal CSA, Srivastava V, Quraishi MA (2017) Application of expired drugs in corrosion inhibition of mild steel. Int J Pharm Chem Anal 4(1):8–12
30. Abdel Hameed RS, Ismail EA, Abu-Nawwas AH, AL-Shafey HI (2015) Expired voltaren drugs as corrosion inhibitor for aluminium in hydrochloric acid. Int J Electrochem Sci 10:2098–2109
31. Garrigues L, Pebere N, Dabosi F (1996) An investigation of the corrosion inhibition of pure aluminum in neutral and acidic chloride solutions. Electrochim Acta 41:1209–1215
32. Totik Y, Sadeler R, Kaymaz I, Gavgali M (2004) The effect of homogenisation treatment on cold deformations of AA 2014 and AA 6063 alloys. J Mater Process Technol 147:60–64
33. Davis JR (1999) Corrosion of aluminium and aluminium alloys. ASM International, Ohio
34. Bai CY, Chou YH, Chao CL, Lee SJ, Ger MD (2008) Surface modifications of aluminum alloy 5052 for bipolar plates using an electroless deposition process. J Power Sour 183:174–181
35. Singh DK, Kumar S, Udayabhanu G, John RP (2016) 4(N,N-dimethylamino) benzaldehyde nicotinic hydrazone as corrosion inhibitor for mild steel in 1 M HCl solution: an experimental and theoretical study. J Mol Liq 216:738–746
36. Alaneme KK, Olusegun SJ, Adelowo OT (2016) Corrosion inhibition and adsorption mechanism studies of *Hunteria umbellata* seed husk extracts on mild steel immersed in acidic solutions. Alexa Eng J 55:673–681
37. Fiori-Bimbi MV, Alvarez PE, Vaca H, Gervasi CA (2015) Corrosion inhibition of mild steel in HCl solution by pectin. Corros Sci 92:192–199
38. Asan A, Soylu S, Kıyak T, Yıldırım F, Öztas SG, Ancın N, Kabasakaloglu M (2006) Investigation on some Schiff bases as corrosion inhibitors for mild steel. Corros Sci 48:3933–3944
39. Njong RN, Ndosiri BN, Nfor EN, Offiong OE (2018) Corrosion inhibitory studies of novel Schiff bases derived from hydralazine hydrochloride on mild steel in acidic media. Open J Phys Chem 8:15–32
40. Yurt A, Duran B, Dal H (2014) An experimental and theoretical investigation on adsorption properties of some diphenolic Schiff bases as corrosion inhibitors at acidic solution/mild steel interface. Arab J Chem 7:732–740
41. Emregul KC, Atakol O (2003) Corrosion inhibition of mild steel with Schiff base compounds in 1 M HCl. Mater Chem Phys 82:188–193
42. Shetty Prakash (2019) Schiff bases: an overview of their corrosion inhibition activity in acid media against mild steel. Chem Eng Commun. https://doi.org/10.1080/00986445.2019.1630387
43. Chaitra TK, Mohana KN, Tandon HC (2018) Evaluation of newly synthesized hydrazones as mild steel corrosion inhibitors by adsorption, electrochemical, quantum chemical and morphological studies. Arab J Basic Appl Sci 25:1–11
44. Dohare P, Quraishi MA, Obot IB (2018) A combined electrochemical and theoretical study of pyridine based Schiff bases as novel corrosion inhibitors for mild steel in hydrochloric acid medium. J Chem Sci 130:1–19
45. Haque J, Srivastava V, Chauhan DS, Lgaz H, Quraishi MA (2018) Microwave-induced synthesis of chitosan Schiff bases and their application as novel and green corrosion

inhibitors: experimental and theoretical approach. ACS Omega 3:5654–5668
46. Jamil DM, Al-Okbi AK, Al-Baghdadi SB, Al-Amiery AA, Kadhim A, Gaaz TS, Kadhum AAH, Mohamad AB (2018) Experimental and theoretical studies of Schiff bases as corrosion inhibitors. Chem Cent J. https://doi.org/10.1186/s13065-018-0376-7
47. Singh DK, Ebenso EE, Singh MK, Behera D, Udayabhanu G, John RP (2018) Non-toxic Schiff bases as efficient corrosion inhibitors for mild steel in 1 M HCl: electrochemical, AFM, FE-SEM and theoretical studies. J Mol Liq 250:88–99
48. Tezcan F, Yerlikaya G, Mahmood A, Kardas G (2018) A novel thiophene Schiff base as an efficient corrosion inhibitor for mild steel in 1.0 M HCl: electrochemical and quantum chemical studies. J Mol Liq 269:398–406
49. Gomma GK, Wahdan MH (1995) Schiff bases as corrosion inhibitors for aluminium in hydrochloric acid solution. Mater Chem Phys 39:209–213
50. Khaled KF, Hackerman N (2003) Investigation of the inhibitive effect of ortho-substituted anilines on corrosion of iron in 0.5 M H_2SO_4 solutions. Mater Chem Phys 82:949
51. Musa AY, Mohamad AB, Kadhum AAH, Takriff MS, Tien LT (2011) Synergistic effect of potassium iodide with phthalazone on the corrosion inhibition of mild steel in 1.0 M HCl. Corros Sci 53:3672
52. Oguzie EE, Li Y, Wang FH (2007) Corrosion inhibition and adsorption behavior of methionine on mild steel in sulfuric acid and synergistic effect of iodide ion. Corros Sci 310:90
53. Fouda AS, Mostafa HA, El-Taib F, Elewady GY (2005) Synergistic influence of iodide ions on the inhibition of corrosion of C-steel in sulphuric acid by some aliphatic amines. Corros Sci 47:1988
54. Dede B, Karipcin F, Arabal F, Cengiz M (2010) Synthesis, structure, and solvent-extraction properties of tridentate oxime ligands and their cobalt(II), nickel(II), copper(II), zinc(II) complexes. Chem Pap 64:25
55. Singh MK, Laskar R, Das A (2002) Synthesis and characterization of ionic heterobimetallic complexes of Ni(II), Cu(II), Zn(II) and Cd(II) ions containing nitrogen and sulphur donors. Ind J Chem Sec A 41:2282
56. Khoo J (2014) Synthesis, characterization and biological activity of two Schiff base ligands and their nickel(II), copper(II), zinc(II) and cadmium(II) complexes derived from S-4-picolyldithiocarbazate and X-ray crystal structure of cadmium(II) complex derived from pyridine-2-carboxaldehyde. Inorg Chim Acta 413:68
57. Silverstein RM, Webster FX, Kiemle DJ (2015) Spectrometric identification of organic compounds, 7th edn. Wiley, New York
58. Chaubey N, Singh VK, Quraishi MA (2017) Electrochemical approach of Kalmegh leaf extract on the corrosion behavior of aluminium alloy in alkaline solution. Inter J Indus Chem 8:75
59. Daoud D, Douadi T, Hamani H, Chafaa S, Noaimi MA (2015) Corrosion inhibition of mild steel by two new S-heterocyclic compounds in 1 M HCl: experimental and computational study. Corros Sci 94:21
60. Hany M, Lateef AE (2015) Experimental and computational investigation on the corrosion inhibition characteristics of mild steel by some novel synthesized imines in hydrochloric acid solutions. Corros Sci 92:104
61. Sanaulla PF, Lokesh HB, Murthy HCA, Raju B (2012) Electrochemical investigation of corrosion inhibition of AA6063 alloy in 1 M hydrochloric acid using Schiff base compounds. J Appl Chem 2:37
62. Bentiss F, Bouanis M, Mernari B, Traisnel M, Vezin H, Lagrenée M (2007) Understanding the adsorption of 4H-1,2,4-triazole derivatives on mild steel surface in molar hydrochloric acid. Appl Surf Sci 253:3696
63. Lebrini M, Lagrenée M, Traisnel M, Gengembre L, Vezin H, Bentiss F (2007) Enhanced corrosion resistance of mild steel in normal sulfuric acid medium by 2,5-bis(n-thienyl)-1,3,4-thiadiazoles: electrochemical, X-ray photoelectron spectroscopy and theoretical studies. Appl Surf Sci 253:9267
64. Tao Z, Zhang S, Li W, Hou B (2009) Corrosion inhibition of mild steel in acidic solution by some oxo-triazole derivatives. Corros Sci 51:2588
65. Zhang S, Tao Z, Li W, Hou B (2009) The effect of some triazole derivatives as inhibitors for the corrosion of mild steel in 1 M hydrochloric acid. Appl Surf Sci 255:6757
66. Oguzie EE, Njoku VO, Enenebeaku CK, Akalezi CO, Obic C (2008) Effect of hexamethyl pararosaniline chloride (crystal violet) on mild steel corrosion in acidic media. Corros Sci 50:3480
67. Doner A, Sahin EA, Kardas G, Serindag O (2013) Investigation of corrosion inhibition effect of 3-[(2-hydroxy-benzylidene)-amino]-2-thioxo-thiazolidin-4-one on corrosion of mild steel in the acidic medium. Corros Sci 66:278
68. Morad MS, Kamal El-Dean AM (2006) 2,2′-Dithiobis(3-cyano-4,6-dimethylpyridine): a new class of acid corrosion inhibitors for mild steel. Corros Sci 48:3398
69. Zhang QB, Hua YX (2009) Corrosion inhibition of mild steel by alkylimidazolium ionic liquids in hydrochloric acid. Electrochim Acta 54:1881
70. Al Hamzi AH, Zarrok H, Zarrouk A, Salghi R, Hammouti B, Al-Deyab SS, Guenoun F (2013) The role of acridin-9(10H)-one in the inhibition of carbon steel corrosion: thermodynamic, electrochemical and DFT studies. Int J Electrochem Sci 8:2586–2605
71. Zhang B, He C, Wang C, Sun P, Li F, Lin Y (2015) Synergistic corrosion inhibition of environment-friendly inhibitors on the corrosion of carbon steel in soft water. Corros Sci 94:6
72. Heydari M, Javidi M (2012) Corrosion inhibition and adsorption behaviour of an amido-imidazoline derivative on API 5L X52 steel in CO_2-saturated solution and synergistic effect of iodide ions. Corros Sci 61:148

Publisher's Note Springer Nature remains neutral with regard to jurisdictional claims in published maps and institutional affiliations.

Affiliations

R. S. Nathiya[1] · Suresh Perumal[2] · Malathy Moorthy[1] · Vajjiravel Murugesan[3] · Rajavel Rangappan[1] · V. Raj[1]

[1] Department of Chemistry, Periyar University, Salem, Tamil Nadu 636011, India

[2] Laboratory for Energy and Advanced Devices (LEAD), Department of Physics and Nanotechnology, SRM Institute of Science and Technology, Kattankulathur, Tamil Nadu, India

[3] Department of Chemistry, B. S. Crescent Abdur Rahman Institute of Science and Technology, Vandalur, Chennai, Tamil Nadu, India